

# Dalton Transactions

Accepted Manuscript



This is an *Accepted Manuscript*, which has been through the Royal Society of Chemistry peer review process and has been accepted for publication.

*Accepted Manuscripts* are published online shortly after acceptance, before technical editing, formatting and proof reading. Using this free service, authors can make their results available to the community, in citable form, before we publish the edited article. We will replace this *Accepted Manuscript* with the edited and formatted *Advance Article* as soon as it is available.

You can find more information about *Accepted Manuscripts* in the [Information for Authors](#).

Please note that technical editing may introduce minor changes to the text and/or graphics, which may alter content. The journal's standard [Terms & Conditions](#) and the [Ethical guidelines](#) still apply. In no event shall the Royal Society of Chemistry be held responsible for any errors or omissions in this *Accepted Manuscript* or any consequences arising from the use of any information it contains.

## ARTICLE

# Exceptionally rapid CO release from a Manganese(I) tricarbonyl complex derived from bis(4-chlorophenylimino)acenaphthene upon exposure to visible light

Cite this: DOI: 10.1039/x0xx00000x

Received 00th January 2012,  
Accepted 00th January 2012

DOI: 10.1039/x0xx00000x

www.rsc.org/

Samantha J. Carrington, Indranil Chakraborty and Pradip K. Mascharak\*

Two manganese (I) carbonyl complexes derived from  $\alpha,\alpha'$ -diimine ligands with extended conjugated framework namely  $[\text{MnBr}(\text{CO})_3(\text{BIAN})]$  (**1**) and  $[\text{MnBr}(\text{CO})_3(\text{MIAN})]$  (**2**), have been synthesized and structurally characterized. Unlike the previously reported photoactive CO-releasing molecules (photoCORMs), these two complexes exhibit unusually high sensitivity toward low power (0.3–10 mW) visible light ( $\lambda \geq 520$  nm) even in the solid state and rapidly release carbon monoxide (CO) upon illumination. The role of the ligand frames in such activity has been examined with the help of theoretical calculations. Application of these photoCORMs in delivering high fluxes of CO to biological targets is anticipated.

## Introduction

Carbon monoxide (CO) is produced endogenously through the break down of heme by the enzyme heme oxygenase (HO).<sup>1</sup> In recent years, CO has been shown to impart anti-inflammatory, anti-apoptotic, and vasoregulatory effects in mammalian tissues. These surprising salutary effects strongly indicate the therapeutic potential of CO derived from endogenous or exogenous generation.<sup>2</sup> In addition, CO exhibits anti-proliferative and pro-apoptotic effects in dysregulated hyperproliferative smooth muscle cells, cancer cells and fibroblasts.<sup>3</sup> Currently, exogenous CO is administered either in the gaseous form or through CO-releasing molecules (CORMs), which have been designed and synthesized to release CO. These CORMs can release CO systemically as it is broken down in vitro and in vivo.<sup>4–6</sup> Further control on the CO release from CORMs can be achieved either by internal triggers such as enzymatic and pH control or through external triggers such as CO release under illumination.<sup>4–6</sup> Metal carbonyl complexes (MCCs) were the first CORMs to be employed for light-triggered CO delivery because of the vast photochemical research available in the literature on CO release and other photochemical processes performed with MCCs derived from ruthenium(II), rhenium(I), manganese(I), and iron(I) in addition to other metals.<sup>7</sup> The first generation of these photoactive carbonyl complexes, used as photoCORMs, include  $\text{Mn}_2(\text{CO})_{10}$  (CORM-1) and  $[\text{Fe}(\text{CO})_5]$  both of which were not soluble in aqueous media and released CO only upon UV light irradiation.<sup>8,9</sup> These proof of concept MCCs however proved that CO could be delivered from a metal carbonyl complex, and that the CO liberated from these MCCs could exhibit many of the same effects seen from inhaled CO.<sup>8</sup>

The first generation photoCORMs were not truly suitable for therapeutic use in biological systems due to the facts that (a) they

require UV illumination for CO release and (b) UV light readily causes damage to tissues. It was realized that the ideal photoCORMs would need to meet certain criteria such as solubility in biological media, stability in media under dark conditions, ability to release CO upon visible light illumination, and must have a non-reactive photoproduct once CO is released.<sup>10–14</sup> Unfortunately, most MCC-based photoCORMs exhibit CO-releasing activity in the UV and near-UV (300–450 nm) region and often lack any absorbance in the visible region.<sup>13</sup> During the past few years, we<sup>15–20</sup> and others<sup>21–23</sup> have focused on MCC-based photoCORMs, that exhibit sensitivity toward visible light and deliver CO to biological targets under controlled conditions. In particular, we have been interested in photoCORMs that exhibit high sensitivity towards visible light in the 500–600 nm range.<sup>17,18</sup> Our design strategy utilizes a combination of a strong  $\sigma$ -donating ancillary ligand like  $\text{Br}^-$  (to destabilize the occupied orbitals) and a coligand with low-lying  $\pi^*$  molecular orbital (MO) to weaken the M–CO bonds in the designed MCCs through a metal-to-ligand charge transfer (MLCT) transition in the visible to near-IR region.<sup>24</sup> The success of this strategy is readily represented by  $[\text{MnBr}(\text{azpy})(\text{CO})_3]$  (azpy = 2-phenylazopyridine, Fig. 1), a photoCORM recently reported by us that rapidly releases CO upon exposure to low-power (10–15 mW/cm<sup>2</sup>) visible light ( $\lambda \geq 520$  nm) with quantum yield value of 0.48.<sup>18</sup>

A close scrutiny of the literature reveals that a variety of MCCs derived from  $\alpha,\alpha'$ -diimine moiety like 2,2'-bipyridine (bpy, Fig. 1) release CO upon illumination with light in the 350–450 nm region.<sup>25</sup> For example,  $[\text{MnBr}(\text{bpy})(\text{CO})_3]$  releases CO when exposed to 420 nm light.<sup>17</sup> We hypothesized that by increasing conjugation in an otherwise bipyridine framework, as in bis(4-chlorophenylimino)acenaphthene (BIAN, Fig. 1), we could further lower the energy level of the  $\pi^*$  MO and induce high sensitivity to visible light. Herein we report  $[\text{MnBr}(\text{CO})_3(\text{BIAN})]$  (**1**), a photoCORM

derived from this  $\alpha,\alpha'$ -diimine ligand with extended conjugated framework and its photophysical properties. For the purpose of comparison, we also report  $[\text{MnBr}(\text{CO})_3(\text{MIAN})]$  (**2**, MIAN = 2-[(4-chlorophenyl)imino]acenaphthylen-1-one, Fig. 1), in which a similar ligand with a N,O donor set has been employed. As described below, the  $\alpha,\alpha'$ -diimine complex **1** with extended  $\pi$ -conjugation does exhibit strong absorbance in the visible region and a higher rate of CO release compared to  $[\text{MnBr}(\text{azpy})(\text{CO})_3]$  upon exposure to visible light ( $\lambda \geq 520$  nm). Interestingly, replacement of one imine-N with O (and removal of one 4-chlorophenyl moiety) in the ligand frame of MIAN affords **2** which displays its visible absorption band in a more red-shifted region and a lower CO release rate under similar conditions. Results of density functional theory (DFT) and time dependent DFT (TDDFT) studies have also been discussed to provide insight into such photochemical behavior.

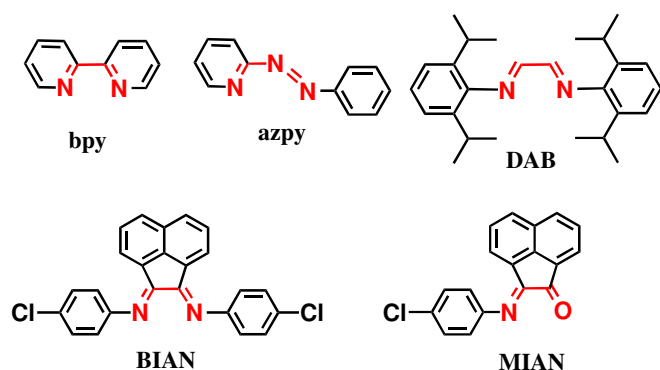


**Figure 1.** Structures of bipyridine (bpy), 2-phenylazopyridine (azpy) and  $N,N'$ -bis(2,6-di-isopropylphenyl)-1,4-diaza-1,3-butadiene ( $\text{Pr}_2\text{Ph-DAB}$ ) (top panel) and Bis(4-chlorophenylimino)acenaphthene (BIAN) and 2-[(4-chlorophenyl)imino]acenaphthylen-1-one (MIAN) (bottom panel).

## Experimental Section

**General:** All reagents were of commercial grade and were used without further purification. The solvents were purified according to the standard procedures.<sup>26</sup> Bis(4-chlorophenylimino)acenaphthene (BIAN) and 2-[(4-chlorophenyl)imino]acenaphthylen-1-one (MIAN) were synthesized following reported procedures.<sup>27,28</sup> The  $^1\text{H}$  NMR spectra were recorded at 298 K on a Varian Unity Inova 500 MHz instrument. A Perkin-Elmer Spectrum-One FT-IR was employed to monitor the IR spectra of the reported compounds. UV-vis spectra were recorded at room temperature using a Varian Cary 5000 UV-Vis-NIR spectrophotometer.

**Synthesis of  $[\text{MnBr}(\text{CO})_3(\text{BIAN})]$  (**1**):** A batch of 178 mg (0.44 mmol) of Bis(4-chlorophenylimino)acenaphthene (BIAN) was dissolved into 10 mL of  $\text{CH}_2\text{Cl}_2$  and was added to a solution (20 mL) of 100 mg (0.36 mmol) of manganese pentacarbonyl bromide in  $\text{CH}_2\text{Cl}_2$  and the mixture was stirred for 26 h at ambient temperature under dinitrogen. The solvent was then removed by evaporation under vacuum and the residue was subsequently washed with hexanes to obtain a deep purple solid in good yield (76%). Single crystals suitable for X-ray diffraction were grown by layering hexanes over a solution of the complex in  $\text{CH}_2\text{Cl}_2$ . Elemental analysis calcd (%) for  $\text{C}_{27}\text{H}_{14}\text{N}_2\text{O}_3\text{Cl}_2\text{Mn Br}$  (620.15): C, 52.29; H, 2.27; N, 4.52; found C, 52.34; H, 2.21; N, 4.49. IR (KBr,  $\text{cm}^{-1}$ ):  $\nu_{\text{CO}}$  = 2026, 1945, 1925;  $^1\text{H}$  NMR ( $\text{CDCl}_3$ ):  $\delta$  = 8.03 (1H), 7.84

(1H), 7.61 (2H), 7.54 (1H), 7.32 (3H), 6.98 (1H);  $\lambda_{\text{max}}$  ( $\text{CH}_2\text{Cl}_2$ )/nm 570 ( $\epsilon/\text{M}^{-1}\text{cm}^{-1}$  4 600), 330 (12 650).

**Synthesis of  $[\text{MnBr}(\text{CO})_3(\text{MIAN})]$  (**2**):** To a solution of 110 mg (0.4 mmol) of manganese pentacarbonyl bromide in 10 mL of  $\text{CH}_2\text{Cl}_2$ , a solution of 120 mg (0.47 mmol) of 2-[(4-chlorophenyl)imino]acenaphthylen-1-one (MIAN) in 10 mL of  $\text{CH}_2\text{Cl}_2$  was added and the mixture was stirred for 24 h under dinitrogen. The blue-green solution was then evaporated to dryness and the residue was washed with hexanes thoroughly to obtain a deep blue-green solid in high yield (80%). X-ray quality crystals were collected by layering hexanes over a solution of the complex in  $\text{CH}_2\text{Cl}_2$ . Elemental analysis calcd (%) for  $\text{C}_{21}\text{H}_{10}\text{NO}_4\text{ClMnBr}$  (510.6): C, 49.39; H, 1.97; N, 2.74; found C, 49.27; H, 2.10; N, 2.68. IR (KBr,  $\text{cm}^{-1}$ ):  $\nu_{\text{CO}}$  = 2028, 1966, 1950;  $^1\text{H}$  NMR ( $\text{CDCl}_3$ ):  $\delta$  = 8.33 (d, 2H), 8.15 (d, 1H), 7.91 (t, 1H), 7.61 (m, 4H), 7.20 (d, 1H);  $\lambda_{\text{max}}$  ( $\text{CH}_2\text{Cl}_2$ )/nm 630 ( $\epsilon/\text{M}^{-1}\text{cm}^{-1}$  3 700), 375 (6 700), 317 (8 400).

## X-ray data collection and structure refinement

Data were collected on a Bruker APEX II single crystal X-ray diffractometer with graphite monochromated Mo  $K\alpha$  radiation ( $\lambda = 0.71073$  Å) by the  $\omega$ -scan technique in the range  $3^\circ \leq 2\theta \leq 48^\circ$  for **1** and  $3^\circ \leq 2\theta \leq 47^\circ$  for **2**. All data were corrected for Lorentz-polarization and absorption.<sup>29</sup> The metal atoms were located from Patterson maps and the rest of the non-hydrogen atoms emerged from successive Fourier syntheses. The structures were then refined by a full-matrix least squares procedure on  $F^2$ . All non-hydrogen atoms were refined anisotropically. All hydrogen atoms were included in calculated positions. The absorption corrections are done using SADABS. Calculations were performed using the SHELXTL™ (V 6.14) program package.<sup>30</sup>

## Photolysis Experiments

CO release from crystals of **1** and **2** was visualized in Paratone™ oil on a glass slide by using a Fiber-Lite MI-150 light source with 150 W lamp (Dolan Jenner Industries). The effective light power on the single crystal was  $3 \text{ mW}/\text{cm}^2$ . Studies on the rates of CO photorelease from the complexes were performed with  $1 \text{ cm} \times 0.4 \text{ cm}$  quartz cuvette. The light source employed in this study consisted of a visible light source (Electro Fiber Optics Corporation, IL 410 illumination system) with a 520 nm cut-off filter to afford low-power visible light ( $10 \text{ mW}/\text{cm}^2$ ). The cuvette was placed at a distance of 1 cm for 1 s intervals of exposure and the electronic absorption spectra were sequentially recorded. Prior to recording each spectrum, the cuvette was inverted to assure sufficient mixing. Apparent rates of CO release ( $k_{\text{CO}}$ ) were determined at an appropriate wavelength for each complex and the logarithm of the complex concentration versus time plots were generated. For quantum yield ( $\phi$ ) measurements, a solution in acetonitrile was used to ensure sufficient absorbance ( $\square 99\%$ ) at the incident wavelength; no more than 10% photolysis occurred in each measurement. Standard actinometry using Reinecke's salt was employed to calibrate the light source (Newport Oriel Apex Illuminator (3 mW power with 1 cm distance at 545 nm)).<sup>31</sup>

## DFT and TDDFT studies

DFT and TDDFT calculations on **1** and **2** were carried out using the double- $\zeta$  basis set 6-31G\* for all atoms with two exceptions: Br, 6-11G\*, and Mn, for which LANL2DZ basis set and effective core potential (ECP) were employed. Calculations were carried out with

the aid of the program PC-GAMESS.<sup>32</sup> The hybrid functional PBE0 was utilized for TDDFT calculations. The X-ray coordinates of **1** and **2** were used as preliminary coordinates for the geometry optimization. The molecular orbitals (MO) were visualized in MacMolPlt for analysis. Oscillation strengths greater than 0.0217 were taken into account for analysis of transitions.

**Table 1.** Crystal data and structure refinement parameters for **1** and **2**

	<b>1</b>	<b>2</b>
Empirical formula	C <sub>27</sub> H <sub>14</sub> N <sub>2</sub> O <sub>3</sub> Cl <sub>2</sub> BrMn	C <sub>21</sub> H <sub>10</sub> NO <sub>4</sub> ClBrMn
FW	620.15	510.60
Temp (K)	296	296
Wavelength (Å)	0.71073	0.71073
Crystal system	monoclinic	Triclinic
Space group	P2(1)/n	P-1
<i>a</i> (Å)	11.4714(8)	8.099(16)
<i>b</i> (Å)	13.0857(10)	8.497(17)
<i>c</i> (Å)	16.9748(12)	16.14(3)
$\alpha$ (deg)	90	77.34(3)
$\beta$ (deg)	92.5820(10)	75.64(2)
$\gamma$ (deg)	90	70.47(3)
<i>V</i> (Å <sup>3</sup> )	2545.5(3)	1003(4)
<i>Z</i>	4	2
Density (calcd)	1.618	1.691
(Mg m <sup>-3</sup> )		
Abs coeff (mm <sup>-1</sup> )	2.331	2.811
No. of unique reflns	4033	2723
<i>R</i> <sub>1</sub>	0.0744	0.0593
<i>wR</i> <sub>2</sub>	0.1835	0.1295
<i>a</i> GOF on <i>F</i> <sup>2</sup>	1.193	0.996

<sup>a</sup>GOF =  $[\sum(w(F_o^2 - F_c^2)^2)/(\sum(N_o - N_c))]^{1/2}$  (*N*<sub>o</sub> = number of observations, *N*<sub>c</sub> = number of variables). <sup>b</sup>*R*<sub>1</sub> =  $\sum ||F_o| - |F_c|| / \sum |F_o|$ . <sup>c</sup> *wR*<sub>2</sub> =  $[(\sum w(F_o^2 - F_c^2)^2) / \sum |F_o|^2]^{1/2}$

## Results and Discussion

### Synthesis and X-ray crystallography

The reaction of [MnBr(CO)<sub>5</sub>] with either bis(4-chlorophenylimino)acenaphthene (BIAN) or 2-[(4-chlorophenyl)imino]acenaphthylene-1-one (MIAN) in CH<sub>2</sub>Cl<sub>2</sub> solution at ambient temperature under dinitrogen afforded **1** and **2** as deep purple and deep blue-green solid respectively. Aluminum foil was employed to exclude light from the reaction mixtures. X-ray diffraction studies confirm distorted octahedral geometry around the Mn(I) center in both complexes with three CO ligands in a *facial* disposition (Fig. 2

and 3). In complex **1**, the reasonably planar equatorial plane is composed of the bidentate BIAN ligand and two equatorial CO ligands (N1, N2, C2, C3) with a mean deviation of 0.0321 Å. The equatorial plane of **2** is similarly comprised of the bidentate MIAN ligand and two CO (N1, O4, C2, C3) with a smaller mean deviation of 0.011 Å. The axial positions in both complexes are occupied by a CO ligand and Br<sup>-</sup>. Close inspection of the bond distances in **1** reveals that the Mn–C1 bond (1.963(15) Å) is significantly longer than that observed in [MnBr(bpy)(CO)<sub>3</sub>] (1.8015(4) Å).<sup>17</sup> In case of **2**, the Mn–C1 bond distance is shorter (1.819(11) Å) and yet somewhat longer than the same bond distance in [MnBr(bpy)(CO)<sub>3</sub>].

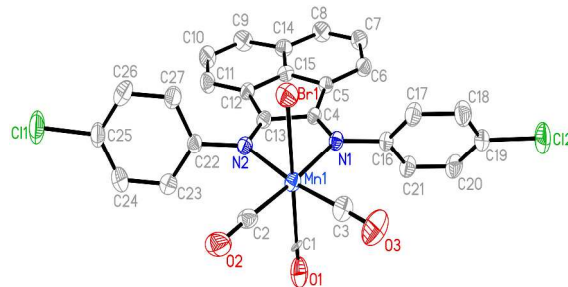


**Figure 2.** Thermal ellipsoid plot of complex **1** shown with 50% probability ellipsoids. Selected bond lengths [Å] molecule **1**: Mn1–C1, 1.963(15); Mn1–C2, 1.808(8); Mn1–C3, 1.810(8); Mn1–N1, 2.063(6); Mn1–N2, 2.056(6); Mn1–Br1, 2.4900(14).

In a recent report, rapid CO photorelease from [MnBr(CO)<sub>3</sub>(<sup>i</sup>Pr<sub>2</sub>Ph-DAB)] (<sup>i</sup>Pr<sub>2</sub>Ph-DAB = (N,N'-bis(2,6-di-isopropylphenyl)-1,4-diaza-1,3-butadiene, Fig. 1), has been attributed to steric crowding in the equatorial plane.<sup>21</sup> Interestingly, the mean Mn–N bond distance in **1** (2.060(6) Å) and the Mn–N1 bond distance in **2** (2.057(7) Å) are comparable to the mean Mn–N distance (2.052(2) Å) in [MnBr(CO)<sub>3</sub>(<sup>i</sup>Pr<sub>2</sub>Ph-DAB)] but longer than the mean Mn–N bond distance (2.043(3) Å) in [MnBr(bpy)(CO)<sub>3</sub>]. Also, the Mn–Br distances in **1** and **2**, 2.490(14) and 2.509(4) Å respectively, are comparable to that observed in [MnBr(CO)<sub>3</sub>(<sup>i</sup>Pr<sub>2</sub>Ph-DAB)] 2.5117(7) Å, and significantly shorter than the Mn–Br distance in [MnBr(bpy)(CO)<sub>3</sub>] (2.538(10) Å). The steric crowding in the coordination sphere of the Mn(I) center in both **1** and **2** is therefore analogous to that reported for [MnBr(CO)<sub>3</sub>(<sup>i</sup>Pr<sub>2</sub>Ph-DAB)].

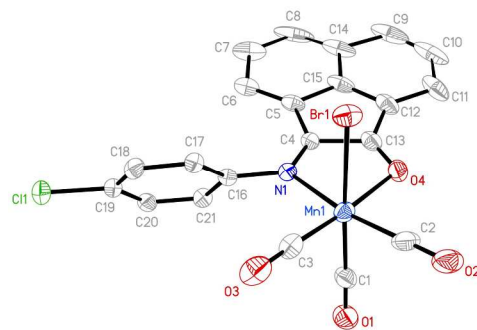


**Figure 3.** Thermal ellipsoid plot of complex **2** shown with 50% probability ellipsoids. Selected bond lengths [Å] Mn1–C1, 1.819(11); Mn1–C2, 1.776(13); Mn1–C3, 1.797(11); Mn1–O4, 2.096(8); Mn1–N1, 2.057(7); Mn1–Br1, 2.509(4).

The acenaphthene fragment of the BIAN ligand in **1** is reasonably planar (mean deviation = 0.0124 Å) while the two phenyl rings are at



orthogonal positions with dihedral angles of 80.7° and 112.2° respectively. In **2**, the dihedral angle between the single phenyl ring and the acenaphthene moiety is 65.6°. The extended structures of **1** and **2** also include significant  $\pi$ -stacking interactions between the acenaphthene fragments and significant intermolecular non-bonding contacts between the Cl atoms on the phenyl ring (Fig. S1 – S4).

### CO release properties

In the solid state, both **1** and **2** are stable when stored in dark. However, unlike the photoCORMs reported by us previously,<sup>15–20</sup> these two carbonyl complexes are *very* sensitive to visible light even in the solid state. The extreme sensitivity to visible light is easily discerned by the copious release of CO upon exposure of the crystalline solids to visible light. A typical example is shown in Fig. 4. In this experiment, a single crystal of **1** was placed in Paratone™ oil under the microscope. When the microscope light (3 mW/cm<sup>2</sup>) was turned on, rapid release of CO was observed as numerous bubbles emerging from the crystal under the oil.

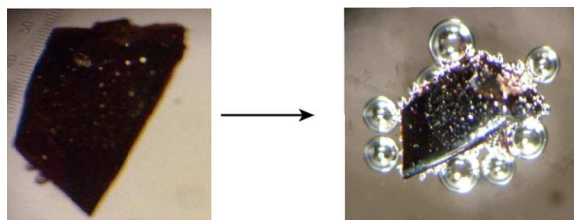


**Figure 4.** CO released from **1** in Paratone™ oil under microscope light (3mW/cm<sup>2</sup>).

Solutions of **1** and **2** in CH<sub>2</sub>Cl<sub>2</sub> are stable for at least 24 h in the absence of light. In coordinating solvents such as acetonitrile (MeCN), dimethylsulfoxide (DMSO), DMSO:water (10:90v/v), **1** also exhibits good stability while **2** releases CO at a slow but steady pace. The electronic absorption spectra of both complexes recorded with solutions (in CH<sub>2</sub>Cl<sub>2</sub>) prepared under dark conditions exhibit two prominent bands. In **1**, the most red-shifted absorption band is centered at 570 nm (Fig. 5). This band arises from an electronic transition from a MO of mostly  $\pi$ -Mn-CO and p-Br character to a

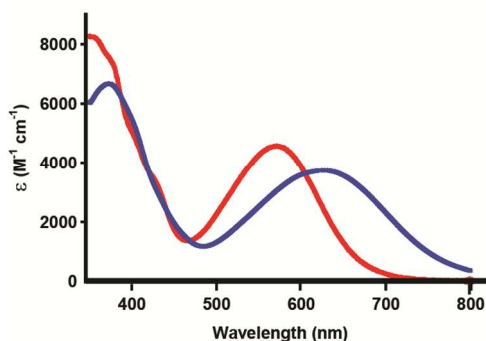


**Figure 5.** Electronic Spectra of **1** (red) and **2** (blue) in CH<sub>2</sub>Cl<sub>2</sub> at 298 K.

MO comprised of the  $\pi^*$  of the organic ligand frame (a metal-to-ligand charge transfer and halide-to-ligand charge transfer MLCT/XLCT transition, *vide infra*). Complex **2** displays its most red-shifted band at 630 nm tailing into 800 nm and is primarily

associated with MLCT/XLCT transition as seen with **1**. The more blue shifted peaks of these two complexes have their origins in  $\pi \rightarrow \pi^*$  transition of the ligand frame in addition to higher energy MLCT transition(s).

Exposure of the solutions of **1** and **2** to visible light brings about rapid changes in their visible absorption spectra as shown in Fig. 6 (and Fig. S5). These spectral changes arise from photorelease of CO upon exposure to light, as evidenced by standard myoglobin assay (data not shown).<sup>18</sup> In the present study, sensitivity of these two carbonyl complexes toward low power (5–15 mW) visible light has been explored and compared with other photoCORMs reported by us

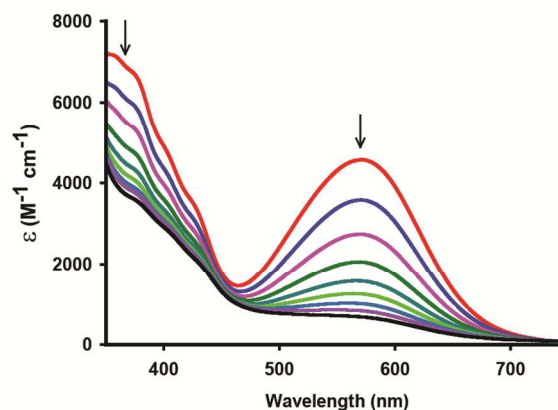


**Figure 6.** Spectral traces of **1** in CH<sub>2</sub>Cl<sub>2</sub> at 298 K upon illumination with low power visible light (15 mW/cm<sup>2</sup>).

and others.<sup>11–23</sup> The super sensitivity of complex **1** is readily evident by its apparent CO release rate ( $k_{CO}$ ) under visible light illumination. When exposed to a broadband visible light source of 15 mW/cm<sup>2</sup> power, **1** afforded a  $k_{CO}$  value of  $25.9 \pm 0.2 \text{ min}^{-1}$  (conc  $1.39 \times 10^{-4} \text{ M}$  in CH<sub>2</sub>Cl<sub>2</sub>) which is much faster than any other photoCORM reported thus far. For example, the rate of CO photorelease of **1** is superior to that for [MnBr(azpy)(CO)<sub>3</sub>] ( $20.9 \pm 0.2 \text{ min}^{-1}$ ) which to date exhibited the most rapid CO photorelease under visible light.<sup>18</sup> Further, **1** exhibits its CO release half-life of 15.2 s under 560 nm monochromatic radiation of exceptionally low power (0.3 mW/cm<sup>2</sup>), a rate surpassing that of [MnBr(CO)<sub>3</sub>(Pr<sub>2</sub>Ph-DAB)] (12 min) under similar illumination as reported by Darendsbourg and coworkers.<sup>21</sup>

In order to examine whether the MLCT/XLCT transition ( $\lambda_{max} = 570 \text{ nm}$ ) is responsible for the fast CO photorelease under visible light, the rate of CO photorelease from **1** in CH<sub>2</sub>Cl<sub>2</sub> has been determined with a visible light source equipped with a cutoff filter ( $\lambda \geq 520 \text{ nm}$ ). In this experimental setting ( $\lambda \geq 520 \text{ nm}$ , CH<sub>2</sub>Cl<sub>2</sub>, conc  $1.25 \times 10^{-4} \text{ M}$ , 10 mW/cm<sup>2</sup>), **1** still exhibited a high  $k_{CO}$  value of  $19.7 \pm 0.2 \text{ min}^{-1}$  indicating a strong correlation between the absorptivity of this carbonyl complex (in the visible region) and its CO photolability. The superior CO photolability of **1** is retained in polar coordinating solvents such as MeCN. For example, the  $k_{CO}$  value of **1** in MeCN (conc  $4.143 \times 10^{-5} \text{ M}$ ) is  $16.9 \pm 0.2 \text{ min}^{-1}$  (for [MnBr(azpy)(CO)<sub>3</sub>],  $k_{CO} = 11.2 \pm 0.1 \text{ min}^{-1}$ ) and the quantum yield value at 545 nm ( $\phi_{545}$ ) is  $0.70 \pm 0.2$ . The comparatively lower absorptivity of **2** (Fig. 5) is presumably responsible for the reduced  $k_{CO}$  values it exhibits in solvents like CH<sub>2</sub>Cl<sub>2</sub>. When exposed to the same broadband visible light (15 mW/cm<sup>2</sup>), a  $k_{CO}$  value of  $11.1 \pm 0.2 \text{ min}^{-1}$  (conc  $5.74 \times 10^{-5} \text{ M}$ ) is obtained. The ability to harvest visible light by photoCORMs is therefore critical provided the visible absorption band is directly involved in labilizing the metal–CO bond(s).<sup>17</sup>

Exhaustive photolysis of a purple solution of **1** in  $\text{CH}_2\text{Cl}_2$  under aerobic conditions results in a pale yellow solution. Upon evaporation, this solution affords a light yellow residue that exhibits no band in the CO stretching frequency region ( $1800\text{--}2200\text{ cm}^{-1}$ ) in its infrared spectrum (Fig. 7). The disappearance of all  $\nu_{\text{CO}}$  bands strongly suggests that prolonged exposure to visible light releases all three CO ligands from complex **1**. In addition, the water extract of the yellow residue displays a six line X-band EPR spectrum

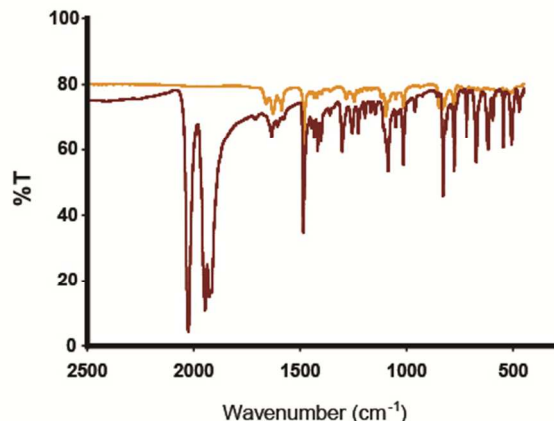


**Figure 7.** Infrared spectra of **1** before (red) and after (yellow) visible light irradiation (KBr disk).

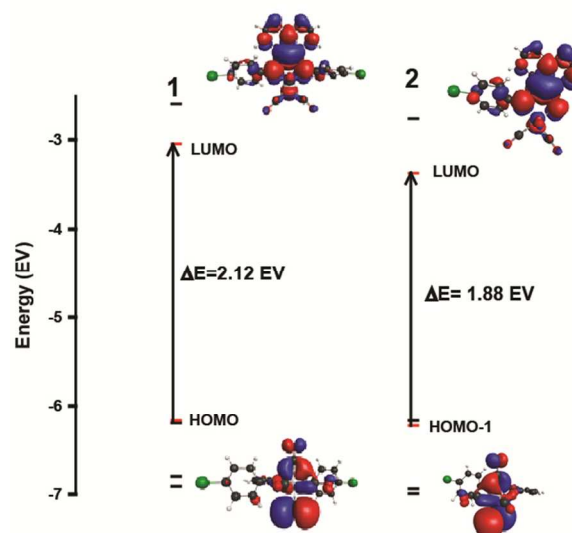
indicative of a Mn(II) aqua complex.<sup>19</sup> It is therefore evident that photolysis of **1** affords free BIAN and a solvated Mn(II) species as photoproducts in addition to three CO molecules.

Density functional theory (DFT) and time-dependent density functional theory (TDDFT) studies have provided insight into the nature of the transitions that promote CO photorelease in **1** and **2**. Both complexes were first geometrically optimized starting from their crystal coordinates and their bond distances and angles were compared to those found in the crystal structure (Table S1). Next, TDDFT calculations were performed to obtain the MO electron densities and the calculated electronic transitions (Table S2). The theoretical spectra of **1** and **2** agreed considerably well with the experimental data.

Complexes **1** and **2** share very similar transitions in the MLCT region as previously elucidated in  $[\text{MnBr}(\text{azpy})(\text{CO})_3]$ .<sup>18</sup> These transitions originate from the occupied orbitals primarily composed of  $\pi(\text{Mn}-\text{CO})$  and  $p\text{-Br}$  and terminate in the LUMO primarily made up of  $\pi^*$ -imine and acenaphthene moiety. Specifically, in **1** about 39% of the highest occupied molecular orbital (HOMO) is composed of  $\pi(\text{Mn}-\text{CO})$  and 25% of  $p\text{-Br}$  bonding character. The lowest unoccupied molecular orbital (LUMO) is primarily composed of  $\pi^*$  ligand frame (77%) and mostly centered on the imine functionalities and acenaphthene moiety (Fig. 8). In case of **2**, the HOMO-1 is comprised of 42%  $\pi(\text{Mn}-\text{CO})$  and 30%  $p\text{-Br}$  bonding character while the  $\pi^*$  orbitals of the acenaphthene and the imine/ketone functionality of the ligand mostly (75%) comprises the LUMO. As seen in Fig. 8, the presence of the ketone-O in the ligand frame of **2** stabilizes the LUMO compared to that in **1** while the occupied HOMO and HOMO-1 in both complexes stay at comparable energy levels. As a consequence, the MLCT band of **2** exhibits a  $\sim 50\text{ nm}$  red shift compared to **1**.

Comprehensive search of the literature reveals that photoCORMs of the type  $[\text{Mn}(\text{L})\text{Br}(\text{CO})_3]$  with  $\text{L} = \alpha,\alpha'$ -diimine ligands (or their analogues) exhibit wide variations in their CO release rates under illumination. In the present work, we have looked closely to the role of the ligand L in selected photoCORMs (Table 2) to understand

how such ligands impart sensitivity to the resulting complexes toward certain ranges of visible light. In case of  $[\text{MnBr}(\text{bpy})(\text{CO})_3]$ , CO photorelease is observed only upon illumination with 420 nm light.<sup>17</sup> When the bpy ligand is replaced with BIAN (a ligand with extended conjugation) in **1**, the MLCT transition is shifted to 570 nm

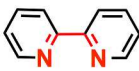
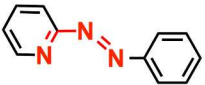
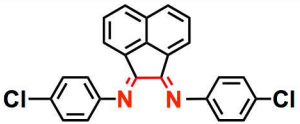
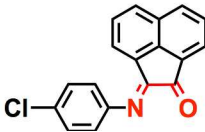


**Figure 8.** Calculated energy diagram of **1** and **2** (left to right). The most prominent MOs involved with transitions under the band associated with CO release under visible light illumination and their compositions are shown.

due to significant stabilization of the LUMO energy level. The occupied HOMO and HOMO-1 levels however remain mostly unchanged due to the high contributions of the  $\pi(\text{Mn}-\text{CO})$  and  $p\text{-Br}$  bonding characters. Interestingly,  $[\text{MnBr}(\text{azpy})(\text{CO})_3]$  and **1** show similarity with respect to the positions of their MLCT bands (590 and 570 nm respectively) despite different extent of conjugation in the ligand frames (Table 2). It appears that the  $\pi$ -acidity of the azo function in the azpy ligand compensates for the observed stabilization of the LUMO and  $[\text{MnBr}(\text{azpy})(\text{CO})_3]$  exhibits high sensitivity toward visible light ( $\lambda \geq 520\text{ nm}$ ,  $\phi = 0.48$ ). It is important to note here that complex **1** is still superior to any photoCORM reported so far due to its high molar absorptivity in the visible region (Table 2). Destabilization of the Mn-CO bond(s) due to steric crowding also enhances CO photolability of **1** similar to  $[\text{MnBr}(\text{CO})_3(\text{Pr}_2\text{Ph-DAB})]$ .<sup>21</sup> Inspection of Table 2 clearly indicate that the ligand L in  $[\text{Mn}(\text{L})\text{Br}(\text{CO})_3]$ -type of photoCORMs plays major roles in (a) shifting the MLCT band position, (b) increasing the molar absorptivity of the resulting complexes, and (c) efficiently utilizing the absorbed energy in promoting CO photorelease (as exemplified by the  $t_{1/2}$  values in Table 2).

The superior CO photolability of **1** in addition to its stability in water/DMSO mixture (90:10 v/v) make this photoCORM a good choice for biological applications. Although **2** exhibits its photoband at 630 nm (compared to 570 nm for **1**), it is unstable in solvents like MeCN and DMSO and hence has limited applications. However both complexes could serve as solids that conveniently deliver small amounts of CO under the control of visible light. To our knowledge no photoCORM with such sensitivity to visible light in the solid state has been reported so far.

**Table 2.** Comparative molar absorptivity (of the MLCT band) and half-lives of CO photorelease of complexes of the type  $[\text{Mn}(\text{L})\text{Br}(\text{CO})_3]$  (L= bpy, azpy, BIAN and MIAN)

L	$\lambda_{\text{max}}$ (nm)	$^a\epsilon (\text{M}^{-1} \text{cm}^{-1})$	$^b t_{1/2}$ (s)
	420	1100	54.9 <sup>c</sup>
	590	3700	3.7
	570	4600	2.1
	630	3700	5.6

<sup>a</sup> Molar absorptivity reported in  $\text{CH}_2\text{Cl}_2$  at 298 K

<sup>b</sup>  $t_{1/2}$  reported in  $\text{CH}_2\text{Cl}_2$  under low power ( $10 \text{ mW/cm}^2$ ) visible light illumination with cutoff filter (520 nm)

<sup>c</sup>  $t_{1/2}$  reported in  $\text{CH}_2\text{Cl}_2$  under low power ( $10 \text{ mW/cm}^2$ ) visible light illumination with cutoff filter (400 nm)

## Conclusion

In summary, the ability to release CO in situ under controlled conditions using visible light may allow photoCORMs to find their place in therapeutic applications. Herein we have sought to further examine the design strategies for relevant photoCORMs that are more sensitive to visible light. Careful choice of ligands has afforded two new photoCORMs **1** and **2** that are highly susceptible to visible light *even in the solid state*. Exposure to low-power visible light causes both complexes to lose CO rapidly. Complex **1** is especially noted for its superior CO photolability with quantum yield value of  $0.70 \pm 0.2$  at 545 nm (power =  $3 \text{ mW/cm}^2$ ). Such control and quick release of CO from **1** could be very useful in rapidly increasing the local CO concentration sometimes required for specific biological applications.

## Acknowledgements

Financial support from the NSF grant DMR-1409335 is gratefully acknowledged.

## Notes and references

Department of Chemistry and Biochemistry, University of California, Santa Cruz, CA 9506, USA. E-mail: pradip@ucsc.edu.

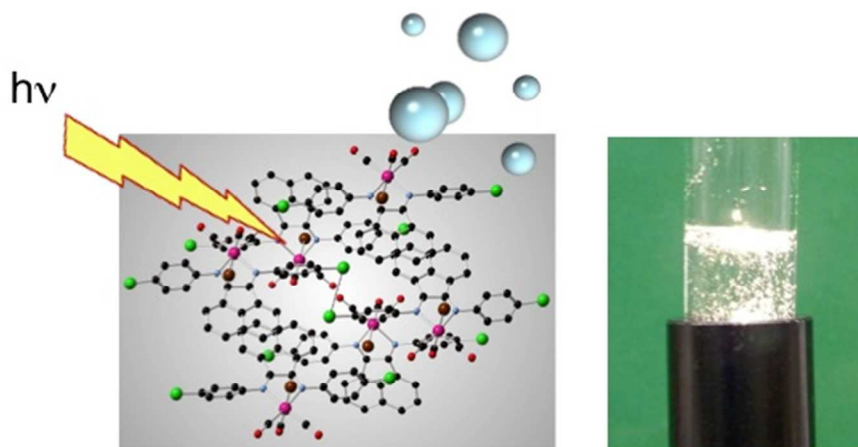
† Electronic Supplementary Information (ESI) available: Packing diagrams of **1** and **2** (Fig. S1-S4), traces of spectral changes of **2** in  $\text{CH}_2\text{Cl}_2$  (Fig. S5), selected bond distances and angles along with optimized DFT bond distances and angles for **1** and **2** (Table S1) and calculated energies, oscillation strengths and nature of transitions for **1** and **2** (Table S2). CCDC 1047275-1047276. For

ESI and crystallographic data in CIF or other electronic format, see DOI: 10.1039/b000000x/.

1. R. Tenhunen, H. S. Marver and R. Schmin, *Proc. Natl. Acad. Sci. USA* 1968, **61**, 748-755.
2. L. Rochette, Y. Cottin, M. Zeller and C. Vergely, *Pharmacol. Therapeut.* 2013, **137**, 133-152.
3. R. Motterlini and L. E. Otterbein, *Nat. Rev. Drug Discov.* 2010, **9**, 728-743.
4. G. J. L. Bernardes and S. García-Gallego, *Angew. Chem. Int. Ed.* 2014, **53**, 9712-9721.
5. M. A. Gonzalez and P. K. Mascharak, *J. Inorg. Biochem.* 2014, **133**, 127-135.
6. U. Schatzschneider, *Br. J. Pharmacol.* 2014, DOI: 10.1111/bph.12688.
7. G. L. Geoffroy and M. S. Wrighton, In *Organometallic Photochemistry*; Academic Press, 1979.
8. R. Foresti, M. G. Bani-Hani and R. Motterlini, *Intensive Care Med.* 2008, **34**, 649-658.
9. R. Motterlini, J. E. Clark, R. Foresti, P. Sarathchandra, B. E. Mann and C. J. Green, *Circ. Res.* 2002, **90**, e17-e24.
10. B. J. Heilman, M. A. Gonzalez and P. K. Mascharak, *Prog. Inorg. Chem.* 2014, **58**, 185-224.
11. S. H. Heinemann, T. Hoshi, M. Westerhausen and A. Schiller, *Chem. Commun.* 2014, **50**, 3644-3660.
12. C. C. Romao, W. S. Blattler, J. D. Seixas and G. J. L. Bernardes, *Chem. Soc. Rev.* 2012, **41**, 3571-3583.
13. R. D. Rimmer, A. E. Pierri and P. C. Ford, *Coord. Chem. Rev.* 2012, **256**, 1509-1519.
14. U. Schatzschneider, *Inorg. Chim. Acta* 2011, **274**, 19-23.
15. M. A. Gonzalez, S. J. Carrington, N. L. Fry, J. L. Martinez and P. K. Mascharak, *Inorg. Chem.* 2012, **51**, 11930-11940.
16. M. A. Gonzalez, S. J. Carrington, I. Chakraborty, M. M. Olmstead and P. K. Mascharak, *Inorg. Chem.* 2013, **52**, 11320-11331.
17. I. Chakraborty, S. J. Carrington and P. K. Mascharak, *ChemMedChem*, 2014, **9**, 1266-1274.
18. S. J. Carrington, I. Chakraborty and P. K. Mascharak, *Chem. Commun.* 2013, 49, 11254-11256.
19. S. J. Carrington, I. Chakraborty, J. M. L. Bernard and P. K. Mascharak, *ACS Med. Chem. Lett.* 2014, **5**, 1324-1328.
20. M. A. Gonzalez, H. Han, A. Moyes, A. Radinos, A. J. Hobbs, N. Coombs, S. R. J. Oliver and P. K. Mascharak, *J. Mater. Chem. B*, 2014, **2**, 2107-2113.
21. V. Yempally, S. J. Kyran, R. K. Raju, W. Y. Fan, E. N. Brothers, D. J. Darensbourg and A. A. Bengali, *Inorg. Chem.* 2014, **53**, 4081-4088.
22. F. Zobi, L. Quaroni, G. Santoro, T. Zlateva, O. Blacque, B. Sarafimov, M. C. Schaub and A. Y. Bogdanova, *J. Med. Chem.* 2013, **56**, 6719-6731.
23. P. Govender, S. Pai, U. Schatzschneider and G. S. Smith, *Inorg. Chem.* 2013, **52**, 5470-5478.
24. I. Chakraborty, S. J. Carrington and P. K. Mascharak, *Acc. Chem. Res.* 2014, **47**, 2603-2611.
25. A. Vlček, Jr. *Coord. Chem. Rev.* 2002, **230**, 225-242.

26. D. D. Perrin and W. L. F. Armarego. Purification of Laboratory Chemicals. 1988, Pergamon Press.
27. H. L. Wong, K. W. Cheng, K. K. Y. Man, C. Y. Kwong, W. K. Chan and A. B. Djurišić. *Proc. SPIE*, 2004, **5520**, 168-175.
28. J. Kovach, M. Peralta, W. W. Brennessel and W. D. Jones. *J. Mol. Struct.* 2011, **992**, 33-38.
29. A. C. T. North, D. C. Philips and F. S. Mathews. *Acta Crystallogr., Sect. C.*, 1968, **24**, 351.
30. SHELXTL™ (V 6.14), G. M. Sheldrick, Bruker Analytical X-ray Systems, Madison, WI, 2000.
31. M. Montalti, A. Credi, L. Prodi and M. T. Gandolfi, In *Handbook of Photochemistry*; Taylor and Francis, 2006.
32. A. V. Nemukhin, B. L. Grigorenko and A. A. Granovsky. *Moscow Univ. Chem. Bull.* 2004, **45**, 75-102.



**Table of Content Figure:**

Both in solid state and in solution, the manganese carbonyl complex  $[\text{MnBr}(\text{CO})_3(\text{BIAN})]$  rapidly releases CO upon illumination with visible light. This photoactive carbonyl complex could find use in delivery of rapid flux of CO to biological targets under the control of light.